Silver Nanoparticles in Heterogeneous Plasmon Mediated Catalysis

María González-Béjar

Abstract Metallic nanoparticles are considered a new class of heterogeneous photocatalysts due to their ability to absorb solar light and convert it into chemical energy. Here, we focus on the use of silver nanoparticles in light driven catalytic processes. This chapter will start with a brief introduction to the currently available nanocomposites that contain silver nanoparticles. Then, the mechanisms behind the photocatalytic activity of those nanocomposites will be discussed.

Keywords Photocatalysis · Heterogeneous plasmon mediated catalysis · Silver nanoparticles

1 Introduction

Light of the appropriate wavelength can selectively activate a desired photocatalyst to generate reactive species that can in turn initiate processes that cannot occur under thermal conditions or that require harsh reagents [1, 2]. Undoubtedly, solar light is considered the greenest reagent for catalytic processes (free and abundant). Photocatalysis is the acceleration of a chemical reaction or transformation produced thanks to the absorption of light by a photocatalyst.

Nowadays, photochemical and photophysical applications have become fundamental for our daily life products: information technology, nanotechnology, sustainable technologies (solar energy storage, waste water cleaning, photovoltaics), lighting (LEDs), etc. [3]. Specifically, photocatalytic applications include advanced oxidation processes (e.g. water decontamination of organic debris) [4, 5], water splitting [6–11], self-cleaning surfaces [12–14], etc.

M. González-Béjar (✉)
Instituto de Ciencia Molecular (ICMol)/Departamento de Química Orgánica, Universidad de Valencia, C/Catedrático José Beltrán 2, 46980 Valencia, Paterna, Spain
e-mail: maria.gonzalez@uv.es

E.I. Alarcon et al. (eds.), *Silver Nanoparticle Applications*, Engineering Materials,
DOI 10.1007/978-3-319-11262-6_4

Metallic nanoparticles (MNPs) possess unique optical, electrical, mechanical, and chemical properties. Thus, their use as photocatalysts to aid in the development of green nanotechnology has attracted a great deal of interest [11, 15–17]. Size reduction increases the Fermi level of the nanoparticle leading to a lower reduction potential of the metal on its surface (see Chap. "Silver Nanoparticles: From Bulk Material to Colloidal Nanoparticles"). The total surface area in nanomaterials is considerably higher than the obtained in the bulk material at the same total concentration. This translates, for example, into higher catalytic performance [18], which is extremely important for catalytic and photocatalytic applications, since one nanoparticle can simultaneously interact with many reactants (comparatively, organic molecules or organometallic complexes only allow one to one interactions) [19].

MNPs upon interaction with an electromagnetic wave give rise to an absorption band known as Surface Plasmon Band (SPB). See Chap. "Silver Nanoparticles: From Bulk Material to Colloidal Nanoparticles" for a detailed explanation. Mahmoud et al. [20]. found that the most active MNPs for catalysis are those with sharp edges, sharp corners, or rough surfaces. The shape of the MNP influences the nature of the surface (facet) exposed to reactants. This would change how reactants and MNP interact and therefore, would influence the outcome of the catalytic processes [21].

This chapter focuses on the use of silver nanoparticles (AgNP) as catalysts. These NPs are also used for other applications such as surface enhanced Raman spectroscopy (Chap. "Surface Enhanced Raman Scattering (SERS) Using Nanoparticles "), single-molecule spectroscopy [22–24], solar cells [25, 26] and biological uses [27] (Chap. "Biomedical Uses of Silver Nanoparticles: From Roman Wine Cups to Biomedical Devices"). For AgNP, a shift in the plasmon absorption band from 400 to 670 nm is observed as the particle shape transitions from a sphere to a cube [11, 28] AgNP' shapes have been found to affect the outcome of the catalytic oxidation of styrene to styrene oxide [29, 30].

MNPs have recently started to be applied in photocatalysis (also called Plasmon Mediated Catalysis, PMC) [11, 31] The use of PMC in synthetic applications is fairly recent and considerable effort is being made to optimize photoreactions promoted by localized plasmons [11, 15–17]. In other words, MNPs are used to transform the energy of light into chemical energy by the formation of short-lived energetic electrons and enhanced electric fields that are generated on the surface and/or in close proximity to the NPs surface [11]. Remarkably, very high-intensity fields have been found in the regions (termed 'hot spots') between plasmonic nanostructures [11].

MNPs interact with the reactant molecules on their surface. Simultaneously, the electrons at their surface can be excited by light. The reaction rate therefore, will depend not only on the number and energy of those electrons, but also on the number of reactant molecules on the NP surface dictated by the affinity between the MNP surface and the reactants [15–17]. Interestingly, plasmonic nanostructures effectively couple thermal and photonic stimuli to drive chemical transformations [32].

For a detailed summary of the essential features of the preparation methods of supported AgNP, the reader is directed to a recent review written by Wang et al. and the references cited therein [17].

Similar to gold nanoparticles, AgNP have optical properties and catalytic capabilities that make them ideal for green photocatalysis (i.e. photocatalysis utilizing visible and ultraviolet light, a major part of the solar spectrum) [15–17]. An ideal green photocatalyst must absorb sunlight (since it is naturally available), must be stable under the reaction conditions (i.e. solvent, or, if there is no other choice, temperature and illumination), must be available, reusable, able to perform selective transformations, and have low toxicity [2].

Photocatalysis is currently used in two particularly beneficial albeit contrasting purposes; (i) pollutant reduction and the destruction of harmful organic pollutants in contaminated water and air using techniques collectively known as advanced oxidation processes (AOPs) [5], and (ii) the synthesis of chemical compounds, "positive photocatalysis", whose aim is to generate new products [33–37].

Several organic compounds, organometallic complexes and semiconductors have been used as photocatalysts in both homogeneous and heterogeneous systems [1, 2]. Colloidal heterogeneous nanocatalysis in particular, refers to those reactions that occur on the surface of nanoparticles [20]. The active site in heterogeneous catalytic reactions is a collection of surface atoms that adsorb reactants and facilitate chemical bond transformation [21]. The loading of nanoparticles on solid supports is a brilliant strategy that is broadening the way of thinking about heterogeneous thermal catalysis and PMC. This chapter will focus on this strategy and its use in PMC.

There are several advantages in using heterogeneous PMC;

(i) MNPs have much better affinity than solid supports to many reactants, especially organic molecules [15].
(ii) MNPs are more resistant to degradation than organic photocatalysts.
(iii) Heterogeneous photocatalysts are easier to remove from the reaction mixture (filtration, centrifugation) than heterogeneous catalysts. This heterogeneity can favor the reaction of one kind of reactant in the presence of others by selective adsorption [1].
(iv) The MNPs get energy from the irradiation source, resulting in high-energy active surface atoms, which is desirable for activating molecules for chemical reactions.
(v) The predictable aggregation of the NPs is prevented by the interaction with the solid support [15].

There are several issues that need to be resolved for the successful application of PMC;

(i) Reshaping of the nanocatalyst during catalysis reaction [21].
(ii) Reaction products deposited on the NP surface could decrease NP stability and limit their recycling.
(iii) The reaction rate may be adversely affected due to the different states of matter in the mixture, or inefficient reactant adsorption/desorption processes, on the solid photocatalysts.

(iv) Reduced availability of active surface area due to NP interaction with the solid support.
(v.) The synthesis of MNPs usually involves reducing agents, organic cappings, and/or growth-directing molecules. Some of those compounds could end up attached to the particle, and thus affect the catalytic process itself [21].
(vi) Particularly in the case of AgNP, it is difficult to prevent the oxidation of AgNP to silver oxide [38].

Despite the above unresolved issues, recent work has demonstrated a plasmonically active and self-regenerative Ag/AgO_x nanostructure to be useful for catalytic reactions and this may open up a new perspective in the field [39]. The support-free catalyst shows plentiful surface-adsorbed oxygen species along with excellent localized surface plasmon resonance (LSPR) and measurable photoluminescence [39].

2 Heterogeneous Photocatalysts Based on AgNP

Semiconductors and insulator supports with surface-embedded metallic nanoparticles for improved stability are being developed and tested. Interestingly, the support can also help in some cases to perform the photocatalytic process, thanks to a synergistic effect generated by the association between the support and the nanoparticle. Accordingly, a thorough understanding of the properties of the new material is required in order to prepare the most efficient photocatalyst possible. Based on the above, research has been carried out on the photocatalytic activity of silver nanoparticles supported on titanium ($AgNP@TiO_2$) [38, 40–44], and other metal oxides (e.g. ZrO_2, SiO_2 and graphene oxide), as well as zeolites [45]. Other metal–semiconductor composite photocatalysts based on the Ag@AgX (X = Cl, Br, I) system have also been developed [17].

It is reasonable to expect different mechanisms for insulator supported AgNP and semiconductor-supported AgNP when applied to photocatalytic processes [15–17]. In this section, we describe these mechanisms in detail to afford the reader with a more in-depth understanding of the photophysical processes required to determine the appropriate strategy for their particular needs. While reviewing these mechanisms, the use of AgNP-based photocatalysis for advances oxidation processes will be briefly summarized and following that, a section focused on positive photocatalysis is presented.

2.1 Heterogeneous Photocatalysts Composed of AgNP and Semiconductors

Semiconductor photocatalysts based on TiO_2 are widely studied for applications in environmental remediation and solar energy conversion [46–49]. Unfortunately,

TiO_2 can only be excited by ultraviolet (UV) light due to its relative wide band gap (3.2 eV). Various strategies have however been developed to make it sensitive to visible light [46–48, 50–57].

Upon illumination of a semiconductor with light, one electron from the conduction band (CB) is promoted to the valence band (VB), leaving behind a vacancy, commonly known as a hole, in the CB [6]. The energy carried by photons from the illumination source has to be greater than the bandgap energy, E_g, (the ΔE between the CB and the VB) for this process to occur. These electron-hole pairs can recombine or be trapped and, most importantly, the photogenerated charge carriers can migrate to the photocatalyst surface and a redox process can take place, giving rise to the corresponding reduced and oxidized products. Some semiconductors respond to visible light (e.g. CdS), allowing scientists to use sunlight or indoor lighting to excite them [2, 58]. Admittedly, the use of photocatalysts based on heavy metals is not the ideal scenario for water and air purification. Thus, in order to overcome this impropriety, several metal-free quantum dots are being developed as potential photocatalysts [59].

A particularly effective strategy for narrowing the band gap of TiO_2 is called defect engineering [55, 60–64]. Introducing oxygen vacancies into the lattice of TiO_2, the light absorption of TiO_2 can be extended to the visible or even infrared region [61, 65]. It is equally important to optimize the photogenerated electron/hole separation characteristics over the TiO_2 surface. Notably, the addition of noble metals to TiO_2 could reduce the photogenerated electron/hole recombination [50, 51, 66].

AgNP supported on TiO_2 (AgNP@TiO_2) have shown photocatalytic activity under UV and visible light and also antibacterial properties [38, 40–43, 67–73]. The ability of AgNP@TiO_2 nanoparticles to degrade phenol [43, 74], methyl red [40], methyl orange (MO) [67] and methylene blue (MB) [38] has been evaluated. An electron transfer reaction takes place upon UV irradiation (Scheme 1) and, where spherical AgNP coated with TiO_2 are concerned, a spectral shift of the plasmon resonance band to a shorter wavelength was detected and elucidated to be due to electron trapping on the AgNP induced by the charge separation after the electron transfer process [40–42]. The interfacial charge transfer between TiO_2 and silver could be enhanced by a negative shift in the Fermi level of the AgNP@TiO_2 composite resulting from the accumulation of electrons produced by the surface plasmon resonance [16].

If an electron acceptor such as thionine dye or oxygen is present, the photogenerated electrons are scavenged and electrons fail to accumulate in the AgNP core [42].

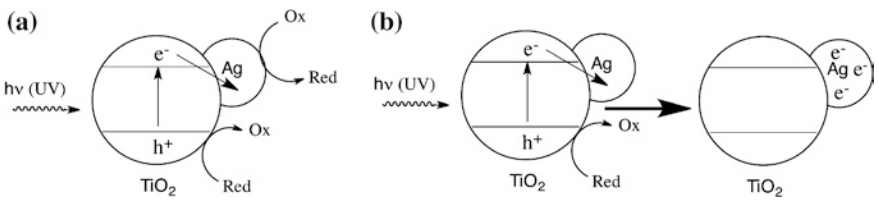

Scheme 1 Proposed mechanism for UV excitation of the AgNP@TiO_2 photocatalyts: **a** semiconductor excitation and electron transfer to AgNP [42, 43] and **b** photoinduced charge separation and charging of the AgNP [41]

This is also the case for Ag@ZnO [75–79]. It is in fact possible to carry out a redox titration and obtain quantitative information about the stored electrons in the Ag@TiO_2 colloids [42]. The capacity of electron storage is determined by the size of the metal core and its ability to undergo charge equilibration with the TiO_2 shell. Once this maximum storage limit is attained, electron-hole recombination in the TiO_2 shell dominates [42].

Electrons accumulated in AgNP can lead to generation of $^{\bullet}O_2^-$ when reacting with O_2, and finally to $^{\bullet}OH$. On the other hand, photogenerated holes in TiO_2 can be scavenged by OH^- or H_2O to generate $^{\bullet}OH$ directly [4, 80]. Moreover, the pH value also dictates the amount of $^{\bullet}OH$ generated [40] and the acidity of the hydroxyl groups on the TiO_2 surface could be enhanced in the presence of AgNP (as described for gold nanoparticles [81]). Thus, AgNP reduce electron-hole pairs recombination and enhance the efficiency of photoreduction owing to the Fermi level equilibration, ultimately leading to a higher yield of $^{\bullet}OH$ [40]. Indeed, due to the electronegativity of AgNP, their Fermi level can shift to negative potentials, resulting in charging effects or original chemical reactivity [82].

Unfortunately, the photo-oxidation of AgNP by O_2 takes place under visible light irradiation of a Ag@TiO_2 film [83] and the photogenerated holes residing on the electron-rich AgNP, drive dissolution of Ag atoms from the AgNP via Ag^+ ejection [84–86]. This can be prevented by either the deposition of TiO_2 made on AgNP, covered with a silica (SiO_2) shell [38], or the preparation of Ag@TiO_2 photocatalyst using Montmorillonite as a support [87]. Either approach effectively prevents the loss of the metal particles during the photocatalytic reaction.

Recently, metal-core@semiconductor-shell nanoparticles consisting of Ag@Cu_2O core-shell were shown to have photocatalytic activity where degradation of MO was concerned. This activity is due to the presence of localized surface plasmon resonance (LSPR) in the AgNP core [88]. This strategy avoids corrosion and dissolution of the metal particles and maximizes the metal—support interaction, thereby facilitating the plasmonic energy transfer processes. Lastly, the local electromagnetic field of the LSPR penetrates the shell, which can be used to tune the center wavelength of the LSPR by changing the shell thickness [88].

2.2 Heterogeneous Photocatalysts Composed of AgNP and Insulator Supports

In 2008, Awazu et al. demonstrated that the photolysis of methylene blue (organic dye) was promoted by a plasmonic effect when visible light was irradiated onto AgNP with a SiO_2 layer placed inside a TiO_2 layer whose plasmon resonance band was near the band edge of TiO_2 [38].

Very recently, AgNP were loaded onto inert supports, which are photocatalytically inactive supports. In this scenario, the charge density is partially localized on the AgNP surface, and this localization is increased by charge separation derived from the LSPR effect [89].

Insulators have different properties than semiconductors since the forbidden band gap between the valence band and conduction band is larger in an insulator, and as a result to this, electrons cannot be promoted from the valence band to the conduction band, even by near UV light [15].

Consequently, when AgNP are deposited onto an insulating oxide, there is no electron transfer between the photo-excited AgNP and the insulator support, and hence, only the nanoparticles participate in the photocatalysis directly [17]. In this case, the photocatalytic activity of noble metal NPs is determined by two factors: the enhanced electromagnetic field of neighboring NPs and the direct interaction of the LSPR excited energetic electrons with reactants. A distinct feature of these systems is that both light absorption and activation of the reactants take place on the AgNP. Charge transfer between the AgNP and support is not required. The particles can be dispersed on an insulating solid (or a very wide band gap semiconductor, such as Al_2O_3 (band gap, 8.0 eV) [90], ZrO_2 [45], SiO_2 (band gap, 9.0 eV) [45, 91], SBA-15 [92], zeolite [45], etc.), which has large specific surface areas and porosity.

The energy of incoming photons is concentrated into small volumes surrounding the AgNP. In fact, a build-up of intense, spatially non-homogeneous oscillating electric fields takes place in the neighborhood of the nanoparticle in the AgNP@insulator nanostructure due to the localize plasmon resonance of AgNP [23, 25, 93]. Hot spots also display very high-intensity fields [94] and these enhanced electric fields play a key role in photocatalysis. Indeed, for nanoparticles smaller than 30 nm, surface plasmons lead to the formation of energetic charge carriers [93, 95], which can be transferred to the surroundings [96] or relaxed by locally heating the nanoparticle [26]. This mechanism is thus quite different from that which occurs in the presence of a semiconductor, where electron transfer between the AgNP and the semiconductor takes place.

AgNP supported on zirconia, silica and Zeolite Y ($Ag@ZrO_2$, $Ag@SiO_2$ and Ag@Zeolite Y) are active photocatalysts for sulforhodamine-B (SRB) and phenol degradation [45]. The degradation of SRB by these photocatalysts increases proportionally with silver content.

Also, $Ag@SiO_2$ exhibited superior photocatalytic performance toward MB photodegradation [91]. Once AgNP are excited, the generation of photo-excited electrons and electron vacancies takes place and are responsible for MB degradation (Scheme 2).

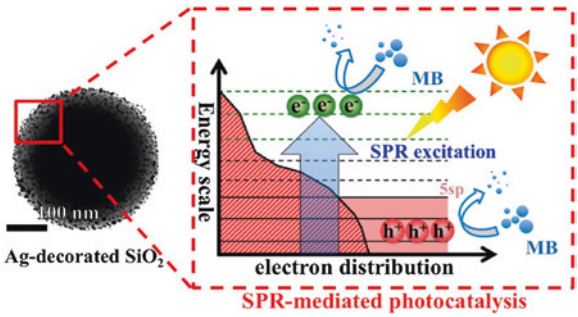

Scheme 2 Schematic diagram illustrating a $AgNP@SiO_2$ nanohybrid that display photocatalytic activity upon surface plasmon resonance (SPR) excitation and degrades methylene blue (MB). Reprinted with permission from Ref. [91]. Copyright 2012 American Chemical Society

Another interesting aspect of photocatalysts containing AgNP is the possible enhancement of the photocatalytic effect of an anchored molecule. For example, core–shell Ag@SiO_2 nanoparticles with an anchored $[Ru(bpy)_3]^{2+}$ dye, showed an enhancement of the photo induced oxidation activity of the ruthenium(II) complex that was attributed to the surface plasmon resonance [97].

2.3 Heterogeneous Photocatalysts Composed of AgNP Ag@AgX (X = Cl, Br)

Silver halides such as AgCl and AgBr are another class of semiconductor supports, which have been extensively used in photographic films due to their photosensitivity. The band gaps, E_g, of AgCl and AgBr are 3.25 and 2.69 eV, respectively [26, 38, 98–100]. Silver halides have been mainly used to host AgNP. Although, the synthesis of silver halide nanostructures has not been as well studied as that of AgNP [101], the synthesis of heterogeneous photocatalysts composed of AgNP Ag@AgX (X = Cl, Br, I) has been extensively investigated over the last decade.

The photocatalytic activity of Ag@AgCl nanoparticles fabricated with different morphological structures was recently shown to extend to visible light due to the SPB of AgNP [102–113]. Various morphotypes of the same NPs have been explored including cubes [106, 109, 112, 113], cubic cages [114], wires [103] films [110] and other shapes [115, 116]. Cubic Ag@AgCl have higher specific surface area, more active sites and facets as compared with spherical counterparts of similar size, all of which are favorable to the enhancement of photocatalytic activity [108]. However, enhanced photocatalytic activities have been reported when using red Ag@AgCl photocatalysts due to their even larger surface area [111].

AgNP supported on AgCl (Ag@AgCl) with high stability and high photocatalytic efficiency under illumination have been used to disinfect water and decompose organic pollutants such as phenol, and the dyes; 2,4-dichlorophenol, methyl orange (MO) [103, 107, 109–114], orange 7 [109], rhodamine B and methylene Blue [106]. These nanocomposites also show reductive activities such as, conversion of CO_2 into liquid carbon fuels (methanol and ethanol) [111, 115] and reduction of Cr^{VI} to Cr^{III} [111, 117].

Upon UV light excitation, a silver halide particle generates an electron-hole pair. The electrons migrate to the surface of the nanoparticle, while the holes migrate to the surface of the AgCl. Subsequently, the photogenerated electron combines with an Ag^+ ion to form an Ag^0 atom [107]. Meanwhile, the photogenerated holes within the silver halide photocatalysts are able to oxidize halide ions to halide atoms (i.e. Cl^- ions to Cl^0 atoms (radicals)), which are strongly oxidative for organic molecules, finally being reduced back to Cl^- ions [107, 109].

The electrons would be trapped by O_2 in solution to form superoxide ions and other reactive oxygen species (ROS) that could also promote the decomposition of dyes [4, 109, 118].

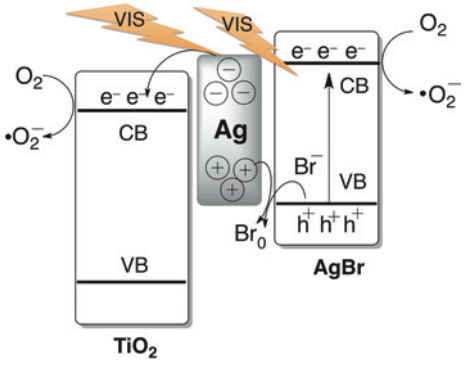

Scheme 3 Schematic diagram for the charge separation in a visible-light irradiated Ag/AgBr/TiO_2 system. Adapted from Ref. [124]

Another similar photocatalyst, AgNP supported on AgBr (Ag@AgBr), catalyzed the decomposition of MO more efficiently than Ag@AgCl under visible light irradiation [116, 119, 120]. Also, reduction of CO_2 to methanol has been observed by plasmon mediated catalysis with Ag@AgBr hexagonal nanoplates [115]. Note AgBr nanoparticles that have shown face-dependent photocatalytic properties for example in the degradation of MO [121]. In this chapter only those semiconductor halides containing AgNP are reviewed. We refer to other papers and the references cited therein for further details on AgX and AgX@semiconductor nanocomposites photocatalytic activity [111, 121].

The photocatalytic activity of Ag@AgI spherical nanoparticles has been recently studied and effectively show antibacterial activity against both E. coli and S. aureus [122]. In all three cases, Ag@AgCl, Ag@AgBr and Ag@AgI plasmon mediated catalysis, the surface of AgX nanoparticles is terminated by X^- ions and therefore, is supposed to be negatively charged [107, 109, 119]. Consequently, AgNP on their surface should polarize the electron distribution such that the regions of its negative charges are far from the Ag/AgX interface, whereas the positive ones are close to it [109]. Then, under visible light illumination, where the SPB of AgNP absorbs, AgNP produce excited electrons and holes [107, 109, 119], thus promoting the photoinduced electron ejection from AgNP into the conduction band of AgX [111, 119]. This is possible because the Fermi energy level of AgX is lower than that of AgNP. Therefore, electrons are transferred from AgNP to AgX until the two systems attain equilibrium and form the new Fermi level [119].

These photogenerated electrons in the conduction band, together with the injected SPR electrons from AgNP, could then initiate the catalytic reaction. Obviously, the interfacial junction between AgNP and AgX could facilitate the charge separation in SPR-excited AgNP and produce long lived charge carriers from the AgNP [119].

As explained above, the holes transferred to the AgX will combine with halide ions X^- ions to form X^0, which will oxidize organic molecules and then reduce back to X^-. In the absence of organic pollutants, X^0 can react with OH^- to form $^\bullet OH$ [109, 123]. The electrons would generate superoxide ions and other reactive oxygen species after reacting with O_2 [111].

2.3.1 Heterogeneous Photocatalysts Composed of AgNP Ag/AgX (X = Cl, Br, I) Loaded on Other Supports

Relevant studies based on this type of photocatalysis mechanism have been widely reported; examples include loaded Ag@AgX (X = halide) hybrid structures on TiO_2 [98, 124–126], Al_2O_3 [100, 127], ZnO [128], BiOBr [129], WO_3 [116], Ag_3VO_4 [130], and graphene (also sulphonated graphene [131] and graphene oxide (GO)) [101, 108, 132].

These nanohybrids have proven useful to degrade organic pollutants such as chlorophenols [100, 124, 127], MO [98, 124, 128, 129], rhodamine B [128, 130], acid orange 7 [124], azo-dyes [125], MB [130], volatile organic compounds (VOCs) in the gas phase (benzene and acetone) [126] and also bacteria [116, 125, 133].

The mechanism that Ag@AgX nanoparticles loaded onto semiconductors undergo upon visible light irradiation is depicted in Scheme 3 (Br and TiO_2 have been chosen as example) [98, 124]. The excited electron was transferred to the conduction band of TiO_2, and a hole was subsequently recovered when the bromide ion and bromide radical were formed.

As discussed above, the oxygen molecule can trap the electron injected into the conduction band of the TiO_2, and form superoxide ions, which promoted the photooxidation reaction. Simultaneously, the highly active bromide radical decomposed the organic molecules near the particles [124].

In another recent contribution, AgNP were used to induce visible light photocatalytic reduction of GO leading to reduced graphene oxide (rGO) in the presence of an electron donor [134]. Indeed, AgNP have also been used as a bridge to connect activated GO and $Ag_2Mo_3O_{10}$ or Ag_3PO_4 [101, 135]. This strategy was also described using Ag@AgX nanoparticles [108, 136–138].

Both, GO or rGO can act as an electron acceptors to effectively suppress the charge recombination, resulting in more reactive species [139]. The advantages of their hybridization can be found in most silver halide and phosphate cases [135–138, 140, 141]. When combined with semiconductors, the photoactivity enhancement of semiconductors after hybridization with rGO or GO has been attributed to a 2D network with an electron sink to accept and shuttle electrons photogenerated in the semiconductors [142–144].

Thus, for $Ag_2Mo_3O_{10}$, a reinforced charge transfer and a suppressed recombination of electron hole pairs result from hybridization of Ag@AgX with GO nanosheets, and contribute to the enhanced photocatalytic activity in the degradation of methyl orange [108].

Silver molibdates such as $Ag_2Mo_3O_{10}$ Ws can also generate an electron/hole pair and to reduce Ag^+ ions to Ag^0 particles under illumination, leading to a cluster of silver atoms on an $Ag_2Mo_3O_{10}$ Ws backbone [101]. However, although they show lower photocatalytic activity than silver salt-based photocatalysts, $Ag@Ag_2Mo_3O_{10}@GO$ nanohybrids are able to photodegrade rhodamine B an 4-chlorophenol [101].

The proposed mechanism for the activity of Ag^0 is as a solid-state electron mediator that accepts electrons from activated GO and $Ag_2Mo_3O_{10}$ Ws (Scheme 4) [101].

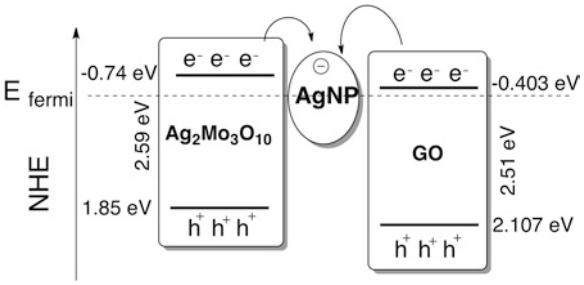

Scheme 4 Photocatalytic process of $Ag@Ag_2Mo_3O_{10}$/activated graphene oxide composite through assistance of solar light. Adapted from reference [101]

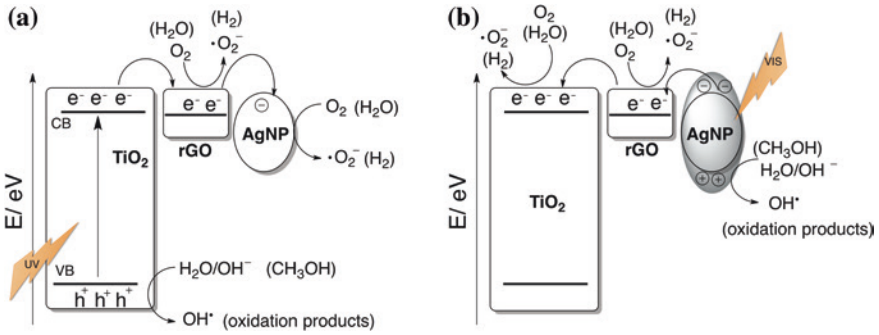

Scheme 5 Proposed mechanism for the photodegradation of RhB and photocatalytic hydrogen production (*in brackets*) by $Ag@rGO@TiO_2$ under **a** UV part and **b** visible part of the simulated sunlight irradiation. Adapted from from reference [145]

Interestingly, Wang et al. [145] have just reported that $Ag@rGO@TiO_2$ nanocomposites can act as photocatalysts to generate hydrogen and are also able to photodegrade RhB. The authors claim that in this system the photogenerated electron separation is improved. Different sizes of AgNP were tested. Small sized AgNP (2–5 nm) could store a photoexcited electron that was generated from TiO_2 leading to photocatalysis improvement; whereas, large sized AgNP were able to absorb visible light. Scheme 5 illustrates the two possible pathways for the photocatalytic process in these $Ag@rGO@TiO_2$ composites.

3 Positive Plasmon Mediated Catalysis

Catalysis is helping to improve chemical conversion, energy production and pollution mitigation. However, most commercial heterogeneous catalytic reactions are being run at relatively high temperatures [90].

Many interesting and useful PMC reactions have been reported using AgNP combined with supports and lower temperatures than their conventional reactions that use only thermal activation [90]. Up to now, water splitting [11], photopolymerization [146–149], isomerization [150], and synthesis of organic compounds [31] have been carried out. Regarding positive PMC, e.g. PMC to make or transform chemicals without destroying them, only CO [90], NH_3 [90] and alcohol oxidations [45, 90, 151], epoxidations [90, 152] and coupling of p-aminobenzenethiol to 4,4'-dimercaptobenzene [112, 153–162] have been explored. Previous examples along this chapter illustrate that most efforts are being devoted to AOPs.

Similar mechanisms for PMC either with AuNPs or AgNP have been described under UV and/or visible light illumination. For AgNP there is an enhanced activity under UV irradiation as compared with visible irradiation, which is sometimes difficult, as explained before, due to the oxidation and/or dissolution of silver. In this chapter, only those examples that use AgNP are mentioned. It is important to remind that: (i) a linear dependence between the temperature and photocatalytic reaction rate at constant light intensity has been observed; (ii) photocatalytic reaction rates on excited MNPs exhibit an intensity dependent transition from the linear to super-linear regime, which indicates an electron-driven chemical reaction [163]. Moreover, this super-linear power law dependence on light intensity takes place at significantly lower intensity than required for super-linear behavior on extended metal surfaces and; (iii) the photocatalytic reaction rate at a given temperature can be obtained by subtracting the rate of the pure thermal process [32]. Readers are strongly recommended to get more insight about linear and super-linear dependences in references [32] and [163] and references cited therein.

After AgNP absorb light, heat is generated and an electron transfer to available adsorbate (reactant) states can occur, forming a negative ion species or a radical. This negative ion can, can either undergo a rapid reaction on the metal surface [90] often referred to as the transient negative ion (TNI) [11, 164–169]; or diffuse to the solution where it could react [45].

This process is very similar to the above-discussed electron injection from an excited AgNP with a nearby semiconductor (i.e. TiO_2, AgX), except that the electron is injected in "adsorbate" states rather than in a semiconductor conduction band [11]. Note that, if the incident light is in the UV range, the formation of charged ion adsorbates could also be initiated by photon-induced interband transition in silver [45].

The interaction of excited plasmons with reactants will be affected by the spatially non-homogeneous distribution of plasmons on the surface of nanoparticles. Therefore, hot spots might play a critical role [11].

Thus, if AgNP are illuminated in the presence of an adsorbate, for example oxygen, the O–O bond is activated at lower temperatures due to a photothermal (electron–phonon driven) elementary step [90]. Scheme 6 contains more detailed information of the formation and subsequent relaxation of the O_2–TNI on the AgNP surface, leading to the dissociation of the adsorbed molecular O_2 [11, 21, 32, 90].

Another mechanism, where a AgNP can transfer electron density to O_2 either directly through chemical interface damping or indirectly through the decay of

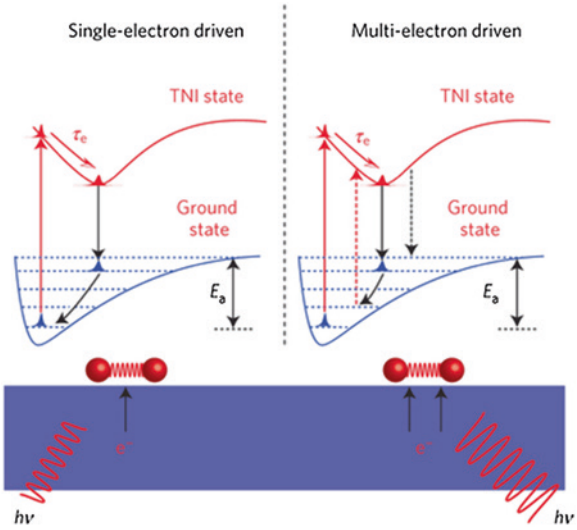

Scheme 6 Proposed molecular mechanism in the linear regime. A single electron excitation deposits vibrational energy into the adsorbate by accelerating the molecule along the TNI potential energy surface (PES) for the lifetime, τ_e. If vibrational energy is not sufficient to overcome the activation barrier, E_a, the adsorbate returns to the thermally equilibrated state. Reprinted with permission from reference [32]. Copyright 2011 Macmillan Publishers Limited

plasmons into energetic electron/hole pairs and subsequent transfer of the e^- to O_2 was proposed by Brus [23]. Irrespective of the mechanism, electrons can transiently populate unoccupied states (orbitals) of adsorbed O_2 and induce electron-mediated O_2 dissociation [23]. Thus, plasmon mediated electron transfer from AgNP to the O_2 $2\pi^*$ orbital forms a transient negative O_2^- species [32, 170, 171].

Factors that influence the capacity of AgNP to drive photocatalytic transformations have been postulated to include:

- (i) temperature-dependent distribution of excited vibrational states, which significantly affects the probability for the plasmon-mediated formation of TNI, and the probability that the TNI will gain sufficient energy to overcome the reaction barrier; and
- (ii) also, much lower activation barriers for chemical transformations on metals as opposed to semiconductors. This allows for lower adsorbate energy required to overcome the activation barrier. Remarkably, Linic et al. suggested that this is the main reason why fairly short-lived TNI on metals (on the order of a few femtoseconds) can induce chemical transformations [11].

AgNP supported on insulators such ZrO_2, Al_2O_3 and SiO_2 or Zeolite Y were found to be highly efficient photocatalysts under visible light for the selective oxidation of benzyl alcohol (Scheme 7, Table 1) [45]. Supports cannot absorb visible light, due to their wide band gaps and there is no electron transfer from the irradiated AgNP to the insulator supports.

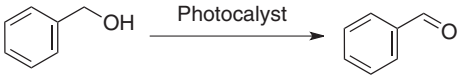

Scheme 7 Oxidation of benzyl alcohol to benzaldehyde

Table 1 Oxidation of benzyl alcohol to benzaldehyde

Photocatalyst	hν	t (h)	Gas	Conversion (%)	Yield (%)
Ag@Zeolite Y	UV	48	Air	11	62
Ag@Zeolite Y	UV	48	O_2	4	100
Ag@TiO_2	Vis	2	O_2	12	12

Ag@TiO_2 with oxygen vacancies gave rise to benzaldehyde under visible light irradiation although better results were reported when using palladium nanoparticles instead of AgNP [51]. The SPB of Ag@TiO_2 cannot be excited with UV. Therefore, upon UV illumination, AgNP on TiO_2 trap the photoexcited electrons from the surface of TiO_2, prolonging the lifetimes of holes and electrons [151]. The holes remaining on the surface of TiO_2 can oxidize absorbed methoxy coming from the thermal dissociation of methanol on TiO_2 to HCHO and HCO. The residual methoxy couples with HCO to form methyl formate [151, 172].

Notably, AgX NPs are also promising materials to reduce CO_2 under visible light irradiation due to the more negative conduction band (CB) edges than $\varphi^{\ominus}(CO_2/CH_3OH)$ and $\varphi^{\ominus}(CO_2/C_2H_5OH)$ (0.38 and 0.085 eV vs. NHE) [111, 112, 115].

Ag@Al_2O_3 nanocomposite has also proven to be an active photocatalyst under visible light irradiation for the selective oxidation (epoxidation) of ethylene to form ethylene oxide (EO), which is a commercially important reaction [32, 90]. The dependence of the photocatalytic rate on the light intensity confirmed that the energetic electrons excited by the LSPR effect of AgNP, directly participate in the photocatalytic process of this oxidation.

Plasmonic excitation of AgNP influences protonation on photoreactions of p-aminobenzenethiol (PATP) leading to its coupling reaction product, 4,4'-dimercaptoazobenzene (DMAB) [153]. In the absence of O_2 or H_2, the plasmon-driven photocatalysis mechanism (hot electron—hole reactions) is the major reaction channel. In the presence of O_2 or H_2, the plasmon-assisted surface catalysis mechanism (activated oxygen/hydrogen reactions) is the major one [154]. Since experimental and theoretical evidence on this surface catalyzed reaction of DMAB produced from PATP, assisted by AgNP in 2010 [173], a series of investigations have been reported to support, or further confirm the conclusions [112, 155–162].

Last but not least, plasmonic mediated water splitting caused by visible light and improvement of photovoltaic devices have attracted attention among scientists [10, 11]. The reader can consult references [10, 11, 38, 174–179] to find more detailed information regarding this topic.

4 Concluding Remarks

MNPs such as AgNP are currently contributing to the development of greener technologies that are based on light driven applications. In this chapter we reviewed several examples of AgNP-support composites that are being used for photocatalysis and plasmon mediated catalytic reactions. Many of them are reusable without losing activity and remain stable under the reaction conditions. Although much effort is being placed in advanced oxidation processes, it is reasonable to assume that significant development will take place in the area of synthetic chemistry promoted by plasmon mediated catalysis. This will allow scientists to utilize the full range of solar energy to activate this new class of photocatalysts for both synthetic and AOPs processes in the near future. This green approach would help to save energy and design more environmentally friendly photocatalytic processes.

Acknowledgments Maria Gonzalez-Bejar thanks the University of Valencia and the Spanish Ministry of Economy and Competitiveness for her Ramón y Cajal contract.

References

1. Galian, R.E., Pérez-Prieto, J.: Catalytic processes activated by light. Energy Environ. Sci. **3**, 1488–1498 (2010)
2. González-Béjar, M., Pérez-Prieto, J., Scaiano, J.C.: Light-driven catalysis. In:Luque, R. (ed.) Green Chemistry, pp. 71–105 Nova Science Publishers, Inc, New York (2012)
3. Klán, P., Wirz, J.: Photochemistry of organic compounds: from concepts to practice. Wiley-Blackwell, Chicester (2009)
4. Hoffmann, M.R., et al.: Environmental applications of semiconductor photocatalysis. Chem. Rev. **95**(1), 69–96 (1995)
5. Khataee, A.R., Fathinia, M.: New and future developments in catalysis: nanoparticle catalysis by surface plasmon, In Sun, S.L. (ed.) Recent advances in photocatalytic processes by nanomaterials, pp. 267–288. Elsevier Science Ltd, United Kingdom (2013)
6. Fujishima, A., Honda, K.: Electrochemical photolysis of water at a semiconductor electrode. Nature **238**, 37–38 (1972)
7. Kudo, A., Miseki, Y.: Heterogeneous photocatalyst materials for water splitting. Chem. Soc. Rev. **38**(1), 253–278 (2009)
8. Zou, Z., et al.: Direct splitting of water under visible light irradiation with an oxide semiconductor photocatalyst. Nature **414**(6864), 625–627 (2001)
9. Borgarello, E., et al.: Photochemical cleavage of water by photocatalysis. Nature **289**(5794), 158–160 (1981)
10. Navarro Yerga, R.M., et al.: Water splitting on semiconductor catalysts under visible-light irradiation. ChemSusChem **2**(6), 471–485, (2009)
11. Linic, S., Christopher, P., Ingram, D.B.: Plasmonic-metal nanostructures for efficient conversion of solar to chemical energy. Nat. Mater. **10**(12), 911–921 (2011)
12. Kafizas, A., et al.: Titanium dioxide and composite metal/metal oxide titania thin films on glass: a comparative study of photocatalytic activity. J. Photochem. Photobiol. A: Chem. **204**(2–3), 183–190 (2009)
13. Giulio, S., et al.: Photo-catalytic coating of polystyrene for household cooling appliances with self cleaning surfaces. J. Appl. Electrochem. **39**(11), 2265–2273 (2009)

14. Bozzi, A., Yuranova, T., Kiwi, J.: Self-cleaning of wool-polyamide and polyester textiles by TiO_2-rutile modification under daylight irradiation at ambient temperature. J. Photochem. Photobiol. A: Chem. **172**(1), 27–34 (2005)
15. Sarina, S., Waclawik, E.R., Zhu, H.: Photocatalysis on supported gold and silver nanoparticles under ultraviolet and visible light irradiation. Green Chem. **15**(7), 1814–1833 (2013)
16. Ueno, K., Misawa, H.: Surface plasmon-enhanced photochemical reactions. J. Photochem. Photobiolo. C: Photochem. Rev. **15**, 31–52 (2013)
17. Wang, P., et al.: Plasmonic photocatalysts: harvesting visible light with noble metal nanoparticles. Phys. Chem. Chem. Phys. **14**(28), 9813–9825 (2012)
18. Eppler, A., et al.: Model catalysts fabricated using electron beam lithography and pulsed laser deposition. J. Phys. Chem. B **101**, 9973–9977 (1997)
19. Goesmann, H., Feldmann, C.: Nanoparticulate functional materials. Angew. Chem. Int. Ed. **49**, 1362–1395 (2010)
20. Mahmoud, M.A., Narayanan, R., El-Sayed, M.A.: Enhancing colloidal metallic nanocatalysis: sharp edges and corners for solid nanoparticles and cage effect for hollow ones. Acc. Chem. Res. **46**(8), 1795–1805 (2013)
21. Linic, S., et al.: Catalytic and photocatalytic transformations on metal nanoparticles with targeted geometric and plasmonic properties. Acc. Chem. Res. **46**(8), 1890–1899 (2013)
22. Nie, S., Emory, S.R.: Probing single molecules and single nanoparticles by surface-enhanced Raman scattering. Science **275**, 1102–1106 (1997)
23. Brus, L.: Noble metal nanocrystals: plasmon electron transfer photochemistry and single-molecule Raman spectroscopy. Acc. Chem. Res. **41**(12), 1742–1749 (2008)
24. Jiang, et al.: Single molecule raman spectroscopy at the junctions of large Ag nanocrystals. J. Phys. Chem. B **107**(37), 9964–9972 (2003)
25. Kelly, K.L., et al.: The optical properties of metal nanoparticles: the influence of size, shape, and dielectric environment. J. Phys. Chem. B **107**(3), 668–677 (2003)
26. Atwater, H.A., Polman, A.: Plasmonics for improved photovoltaic devices. Nat. Mater. **9**(3), 205–213 (2010)
27. Jain, P.K., et al.: Noble metals on the nanoscale: optical and photothermal properties and some applications in imaging, sensing, biology, and medicine. Acc. Chem. Res. **41**(12), 1578–1586 (2008)
28. Stamplecoskie, K.G., Scaiano, J.C.: Light emitting diode irradiation can control the morphology and optical properties of silver nanoparticles. J. Am. Chem. Soc. **132**, 1825–1827 (2010)
29. Chimentão, R.J., et al.: Different morphologies of silver nanoparticles as catalysts for the selective oxidation of styrene in the gas phase. Chem. Commun. pp. 846–847 (2004)
30. Xu, R., et al.: Shape-dependent catalytic activity of silver nanoparticles for the oxidation of styrene. Chem. Asian J. **1**, 888–893 (2006)
31. Sun, M., New and Future Developments in Catalysis: Nanoparticle Catalysis by Surface Plasmon, In: Sun, S.L. (ed.) Catalysis Nanoparticles, pp. 473–487 Elsevier Science Ltd, United Kingdom (2013)
32. Christopher, P., et al.: Singular characteristics and unique chemical bond activation mechanisms of photocatalytic reactions on plasmonic nanostructures. Nat. Mater. **11**(12), 1044–1050 (2012)
33. Corma, A., et al.: Photoinduced electron transfer within zeolite cavities: cis-stilbene isomerization photosensitized by 2,4,6-Triphenylpyrylium cation imprisoned inside zeolite Y. J. Am. Chem. Soc. **116**, 2276–2280 (1994)
34. Corma, A., García, H.: Zeolite-based photocatalysts. Chem. Commun. **13**, 1443–1459 (2004)
35. Protti, S., Fagnoni, M.: The sunny side of chemistry: green synthesis by solar light. Photochem. Photobiol. Sci. **8**, 1499–1516 (2009)
36. Palmisano, G., et al.: Photocatalysis: a promising route for 21st century organic chemistry. Chem. Commun. pp. 3425–3437 (2007)
37. Esser, P., Pohlmann, B., Scharf, H.-D.: The photochemical synthesis of fine chemicals with sunlight. Angew. Chem. Int. Ed. **33**, 2009–2023 (1994)
38. Awazu, K., et al.: A Plasmonic photocatalyst consisting of silver nanoparticles embedded in titanium dioxide. J. Am. Chem. Soc. **130**(5), 1676–1680 (2008)

39. Zhao, Z., Carpenter, M.A.: Support-free bimodal distribution of plasmonically active Ag/AgOx nanoparticle catalysts: attributes and plasmon enhanced surface chemistry. J. Phys. Chem. C **117**(21), 11124–11132 (2013)
40. Petronella, F., et al.: Photocatalytic activity of nanocomposite catalyst films based on nanocrystalline metal/semiconductors. J. Phys. Chem. C **115**(24), 12033–12040 (2011)
41. Hirakawa, T., Kamat, P.V.: Photoinduced electron storage and surface plasmon modulation in Ag@TiO_2 clusters. Langmuir **20**, 5645–5647 (2004)
42. Hirakawa, T., Kamat, P.V.: Charge separation and catalytic activity of Ag@TiO_2 core-shell composite clusters under UV-irradiation. J. Am. Chem. Soc. **127**(11), 3928–3934 (2005)
43. Grabowska, E., et al.: Modification of titanium(IV) dioxide with small silver nanoparticles: application in photocatalysis. J. Phys. Chem. C **117**(4), 1955–1962 (2013)
44. Gong, D., et al.: Silver decorated titanate/titania nanostructures for efficient solar driven photocatalysis. J. Solid State Chem. **189**, 117–122 (2012)
45. Chen, X., et al.: Supported silver nanoparticles as photocatalysts under ultraviolet and visible light irradiation. Green Chem. **12**(3), 414–419 (2010)
46. Chen, X., et al.: Increasing solar absorption for photocatalysis with black hydrogenated titanium dioxide nanocrystals. Science **331**, 746–750 (2011)
47. Chen, X., Mao, S.S.: Titanium dioxide nanomaterials: synthesis, properties, modifications, and applications. Chem. Rev. **107**, 2891–2959 (2007)
48. Zhang, Y., et al.: TiO_2 − graphene nanocomposites for gas-phase photocatalytic degradation of volatile aromatic pollutant: is TiO_2 − graphene truly different from other TiO_2 − carbon composite materials? ACS Nano **4**, 7303–7314 (2010)
49. Hoang, S., et al.: enhancing visible light photo-oxidation of water with TiO_2 nanowire arrays via cotreatment with H_2 and NH_3: synergistic effects between Ti^{3+} and N. J. Am. Chem. Soc. **134**, 3659–3662 (2012)
50. Zhang, N., et al.: Synthesis of M@TiO_2 (M = Au, Pd, Pt) core − shell nanocomposites with tunable photoreactivity. J. Phys. Chem. C **115**, 9136–9145 (2011)
51. Pan, X., Xu, Y.-J.: Defect-mediated growth of noble-metal (Ag, Pt, and Pd) nanoparticles on TiO_2 with oxygen vacancies for photocatalytic redox reactions under visible light. J. Phys. Chem. C **117**(35), 17996–18005 (2013)
52. Xu, Y.-J., Zhuang, Y., Fu, X.: New insight for enhanced photocatalytic activity of TiO_2 by doping carbon nanotubes: a case study on degradation of benzene and methyl orange. J. Phys. Chem. C **114**, 2669–2676 (2010)
53. Kumar, S.G., Devi, L.G.: Review on modified TiO_2 photocatalysis under UV/visible light: selected results and related mechanisms on interfacial charge carrier transfer dynamics. J. Phys. Chem. A **115**, 13211–13241 (2011)
54. Li, R., Kobayashi, H., Guo, J.F., Fan, J.: Visible-Light-Driven Surface Reconstruction of Mesoporous TiO_2: toward visible-light absorption and enhanced photocatalytic activities. Chem. Commun. **47**, 8584–8586 (2011)
55. Zuo, F., et al.: Self-Doped Ti^{3+} enhanced photocatalyst for hydrogen production under visible light. J. Am. Chem. Soc. **132**, 11856–11857 (2010)
56. Zhang, N., et al.: Constructing ternary CdS − Graphene − TiO_2 hybrids on the flatland of graphene oxide with enhanced visible-light photoactivity for selective transformation. J. Phys. Chem. C **116**, 18023–18031 (2012)
57. Zhang, Y., et al.: Engineering the unique 2D mat of graphene to achieve graphene-TiO_2 nanocomposite for photocatalytic selective transformation: what advantage does graphene have over its forebear carbon nanotube? ACS Nano **5**, 7426–7435 (2011)
58. Kim, H.G., et al.: Photocatalytic nanodiodes for visible-light photocatalysis. Angew. Chem. Int. Ed. **44**, 4585–4589 (2005)
59. Ding, C., Zhu, A., Tian, Y.: Functional surface engineering of C-dots for fluorescent biosensing and in vivo bioimaging. Acc. Chem. Res. **47**(1), 20–30 (2014)
60. Cronemeyer, D.C.: Infrared absorption of reduced rutile TiO_2 single crystals. Phys. Rev. **113**, 1222–1226 (1959)
61. Pan, X., et al.: Defective TiO_2 with oxygen vacancies: synthesis, Properties and photocatalytic Applications. Nanoscale **5**, 3601–3614 (2013)

62. Hoang, S., Guo, S., Mullins, C.B.: Coincorporation of N and Ta into TiO_2 nanowires for visible light driven photoelectrochemical water oxidation. J. Phys. Chem. C **116**, 23283–23290 (2012)
63. Hoang, S., et al.: Visible light driven photoelectrochemical water oxidation on nitrogen-modified TiO_2 nanowires. Nano Lett. **12**, 26–32 (2011)
64. Justicia, I., et al.: Designed self-doped titanium oxide thin films for efficient visible-light photocatalysis. Adv. Mater. **14**, 1399–1402 (2002)
65. Pan, X., et al.: Selective oxidation of benzyl alcohol over TiO_2 nanosheets with exposed 001 facets: catalyst deactivation and regeneration. Appl. Catal. A **453**, 181–187 (2013)
66. Ye, M., et al.: High-efficiency photoelectrocatalytic hydrogen generation enabled by palladium quantum dots-sensitized TiO_2 nanotube arrays. J. Am. Chem. Soc. **134**, 15720–15723 (2012)
67. Arabatzis, I.M., et al.: Silver-modified titanium dioxide thin films for efficient photodegradation of methyl orange. Appl. Catal. B- Environ. **42**(2), 187–201 (2003)
68. Ji, Z., et al.: The role of silver nanoparticles on silver modified titanosilicate ETS-10 in visible light photocatalysis. Appl. Catal. B: Environ. **102**, 323–333 (2011)
69. Stathatos, E., et al.: Photocatalytically deposited silver nanoparticles on mesoporous TiO_2 films. Langmuir **16**(5), 2398–2400 (2000)
70. Smirnova, N., et al.: Photoelectrochemical and photocatalytic properties of mesoporous TiO_2 films modified with silver and gold nanoparticles. Surf. Interface Anal. **42**(6–7), 1205–1208 (2010)
71. Liu, S.X., et al.: A mechanism for enhanced photocatalytic activity of silver-loaded titanium dioxide. Catal. Today **93–95**, 877–884 (2004)
72. Messaoud, M., et al.: Photocatalytic generation of silver nanoparticles and application to the antibacterial functionalization of textile fabrics. J. Photochem. Photobiol. A: Chem. **215**, 147–156 (2010)
73. Ingram, D.B., et al.: Predictive model for the design of plasmonic metal/semiconductor composite photocatalysts. ACS Catal. **1**(10), 1441–1447 (2011)
74. Zheng, Z., et al.: Facile in situ synthesis of visible-light plasmonic photocatalysts $M@TiO_2$ ($M = Au, Pt, Ag$) and evaluation of their photocatalytic oxidation of benzene to phenol. J. Mater. Chem. **21**, 9079–9087 (2011)
75. Wood, A., Giersig, M., Mulvaney, P.: Fermi level equilibration in quantum dot-metal nanojunctions. J. Phys. Chem. B **105**, 8810–8815 (2001)
76. Georgekutty, R., Seery, M.K., Pillai, S.C.: A highly efficient Ag-ZnO photocatalyst: synthesis, properties, and mechanism. J. Phys. Chem. **112**(35), 13563–13570 (2008)
77. Zheng, Y., et al.: Ag/ZnO heterostructure nanocrystals: synthesis, characterization, and photocatalysis. Inorg. Chem. **46**(17), 6980–6986 (2007)
78. Zheng, Y., et al.: Photocatalytic activity of Ag/ZnO heterostructure nanocatalyst: correlation between structure and property. J. Phys. Chem. C **112**(29), 10773–10777 (2008)
79. Liu, H.R., et al.: Worm-like Ag/ZnO core, shell heterostructural composites: fabrication, characterization, and photocatalysis. J. Phys. Chem. C **116**(30), 16182–16190 (2012)
80. Goto, H., et al.: Quantitative analysis of superoxide ion and hydrogen peroxide produced from molecular oxygen on photoirradiated TiO_2 particles. J. Catal. **225**, 223–229 (2004)
81. Subramanian, V., Wolf, E., Kamat, P.V.: Semiconductor, àímetal composite nanostructures. to what extent do metal nanoparticles improve the photocatalytic activity of TiO_2 films? J. Phys. Chem. B **105**(46), 11439–11446 (2001)
82. Henglein, A., Holzwarth, A., Mulvaney, P.: Fermi level equilibration between colloidal lead and silver particles in aqueous solution. J. Phys. Chem. **96**(22), 8700–8702 (1992)
83. Ohko, Y., et al.: Multicolour photochromism of TiO_2 films loaded with silver nanoparticles. Nat. Mater. **2**(1), 29–31 (2003)
84. Kelly, K.L., Yamashita, K.: The optical properties of metal nanoparticles: the influence of size, shape, and dielectric environment. J. Phys. Chem. B **110**, 7743–7749 (2006)
85. Matsubara, K., et al.: Plasmon resonance-based photoelectrochemical tailoring of spectrum, morphology and orientation of Ag nanoparticles on TiO_2 single crystals. J. Mater. Chem. **19**(31), 5526–5532 (2009)

86. Matsubara, K., et al.: Effects of adsorbed water on plasmon-based dissolution, redeposition and resulting spectral changes of Ag nanoparticles on single-crystalline TiO_2. Phys. Chem. Chem. Phys. **10**(16), 2263–2269 (2008)
87. Wu, T.-S., et al.: Montmorillonite-supported Ag/TiO_2 nanoparticles: an efficient visible-light bacteria photodegradation material. ACS Appl. Mater. Interfaces **2**(2), 544–550 (2010)
88. Li, J., et al.: Ag@Cu_2O Core-shell nanoparticles as visible-light plasmonic photocatalysts. ACS Catal. **3**(1), 47–51 (2013)
89. Stepanov, A.L., Xiao, X., Ren, F., Kavetskyy, T., Osin, Y.N.: Catalytic and biological sensitiviy of TiO_2 and SiO_2 matrices with silver nanoparticles created by ion implantation: a review. Rev. Adv. Mater. Sci. **34**, 107−122 (2013)
90. Christopher, P., Xin, H., Linic, S.: Visible-light-enhanced catalytic oxidation reactions on plasmonic silver nanostructures. Nat. Chem. **3**(6), 467–472 (2011)
91. Chen, K.-H., et al.: Ag-Nanoparticle-decorated SiO_2 nanospheres exhibiting remarkable plasmon-mediated photocatalytic properties. J. Phys. Chem. C **116**(35), 19039–19045 (2012)
92. Fuku, K., et al.: The synthesis of size- and color-controlled silver nanoparticles by using microwave heating and their enhanced catalytic activity by localized surface plasmon resonance. Angew. Chem. Int. Ed. **52**(29), 7446–7450 (2013)
93. Burda, C., et al.: Chemistry and properties of nanocrystals of different shapes. Chem. Rev. **105**(4), 1025–1102 (2005)
94. Gunnarsson, L., et al.: Confined plasmons in nanofabricated single silver particle pairs: experimental observations of strong interparticle interactions. J. Phys. Chem. B **109**(3), 1079–1087 (2004)
95. Evanoff, D.D., Chumanov, G.: Synthesis and optical properties of silver nanoparticles and arrays. ChemPhysChem **6**(7), 1221–1231 (2005)
96. Kamat, P.V.: Photophysical, photochemical and photocatalytic aspects of metal nanoparticles. J. Phys. Chem. B **106**(32), 7729–7744 (2002)
97. Mori, K., et al.: Enhancement of the photoinduced oxidation activity of a ruthenium(II) complex anchored on silica-coated silver nanoparticles by localized surface plasmon resonance. Angew. Chem. Int. Ed. **49**(46), 8598–8601 (2010)
98. Yu, J., Dai, G., Huang, B.: Fabrication and characterization of visible-light-driven plasmonic photocatalyst Ag/AgCl/TiO_2 nanotube arrays. J. Phys. Chem. C **113**(37), 16394–16401 (2009)
99. Glaus, S., Calzaferri, G.: The band structures of the silver halides AgF, AgCl, and AgBr: a comparative study. Photochem. Photobiol. Sci. **2**, 398–401 (2003)
100. Hu, C., et al.: Plasmon-induced photodegradation of toxic pollutants with Ag-AgI/Al_2O_3 under visible-light irradiation. J. Am. Chem. Soc. **132**(2), 857–862 (2010)
101. Zhang, K., et al.: Chemically modified graphene oxide-wrapped quasi-micro Ag decorated silver trimolybdate nanowires for photocatalytic applications. J. Phys. Chem. C **117**(45), 24023–24032 (2013)
102. Wang, P., et al.: Synthesis of highly efficient Ag@AgCl plasmonic photocatalysts with various structures. Chem. - Eur. J. **16**(2), 538–544 (2008)
103. Bi, Y., Ye, J.: In situ oxidation synthesis of Ag/AgCl core-shell nanowires and their photocatalytic properties. Chem. Commun. **43**, 6551–6553 (2009)
104. Li, Y., Ding, Y.: Porous AgCl/Ag nanocomposites with enhanced visible light photocatalytic properties. J. Phys. Chem. C **114**(7), 3175–3179 (2010)
105. Lou, Z., et al.: The synthesis of the near-spherical AgCl crystal for visible light photocatalytic applications. Dalton Trans. **40**(16), 4104–4110 (2011)
106. An, C., Peng, S., Sun, Y.: Facile synthesis of sunlight-driven AgCl:Ag plasmonic nanophotocatalyst. Adv. Mater. **22**(23), 2570–2574 (2010)
107. Wang, P., et al.: Ag@AgCl: A highly efficient and stable photocatalyst active under visible light. Angew. Chem. Int. Ed. **47**(41), 7931–7933 (2008)
108. Zhu, M., Chen, P., Liu, M.: Graphene oxide enwrapped Ag/AgX (X = Br, Cl) nanocomposite as a highly efficient visible-light plasmonic photocatalyst. ACS Nano **5**(6), 4529–4536 (2011)

109. Dong, R., et al.: Ecofriendly synthesis and photocatalytic activity of uniform cubic Ag@AgCl plasmonic photocatalyst. J. Phys. Chem. C **117**(1), 213–220 (2013)
110. Han, L., et al.: Facile synthesis of a free-standing Ag@AgCl film for a high performance photocatalyst and photodetector. Chem. Commun. **49**(43), 4953–4955 (2013)
111. Cai, B., et al.: A distinctive red Ag/AgCl photocatalyst with efficient photocatalytic oxidative and reductive activities. J. Mater. Chem. A **2**(15), 5280–5286 (2014)
112. Wu, D.-Y., et al.: Photon-driven charge transfer and photocatalysis of p-aminothiophenol in metal nanogaps: a DFT study of SERS. Chem. Commun. **47**(9), 2520–2522 (2011)
113. Han, L., et al.: Facile solvothermal synthesis of cube-like Ag@AgCl: a highly efficient visible light photocatalyst. Nanoscale **3**(7), 2931–2935 (2011)
114. Tang, Y., et al.: Efficient Ag@AgCl cubic cage photocatalysts profit from ultrafast plasmon-induced electron transfer processes. Adv. Funct. Mater. **23**(23), 2932–2940 (2013)
115. An, C., et al.: Strongly visible-light responsive plasmonic shaped AgX:Ag (X = Cl, Br) nanoparticles for reduction of CO_2 to methanol. Nanoscale **4**(18), 5646–5650 (2012)
116. Wang, P., et al.: Ag/AgBr/$WO_3 \cdot H_2O$: Visible-Light photocatalyst for bacteria destruction. Inorg. Chem. **48**(22), 10697–10702 (2009)
117. Wang, P., et al.: Highly efficient visible light plasmonic photocatalysts Ag@Ag(Cl, Br) and Ag@AgCl-AgI. ChemCatChem **3**(2), 360–364 (2011)
118. Soni, S.S., et al.: Visible-light photocatalysis in titania-based mesoporous thin films. Adv. Mater. **20**(8), 1493–1498 (2008)
119. Jiang, J., Li, H., Zhang, L.: New insight into daylight photocatalysis of AgBr@Ag: synergistic effect between semiconductor photocatalysis and plasmonic photocatalysis. Chem. - Eur. J. **18**(20), 6360–6369 (2012)
120. Wang, H., et al.: Polyhedral AgBr microcrystals with an increased percentage of exposed 111 facets as a highly efficient visible-light photocatalyst. Chem. - Eur. J. **18**(15), 4620–4626 (2012)
121. Wang, H., et al.: Facet-dependent photocatalytic properties of AgBr nanocrystals. Small **8**(18), 2802–2806 (2012)
122. Ghosh, S., et al.: Ag@AgI, Core@Shell structure in agarose matrix as hybrid: synthesis, characterization, and antimicrobial activity. Langmuir **28**(22), 8550–8561 (2012)
123. Lu, M.-C., Chen, J.-N., Chang, C.-P.: Effect of inorganic ions on the oxidation of dichlorvos insecticide with Fenton's reagent. Chemosphere **35**(10), 2285–2293 (1997)
124. Dong, R., et al.: AgBr@Ag/TiO_2 core-shell composite with excellent visible light photocatalytic activity and hydrothermal stability. Catal. Commun. **38**, 16–20 (2013)
125. Hu, C., et al.: Ag/AgBr/TiO_2 Visible light photocatalyst for destruction of azodyes and bacteria. J. Phys. Chem. B **110**(9), 4066–4072 (2006)
126. Zhang, Y., et al.: Nanocomposite of Ag-AgBr-TiO_2 as a photoactive and durable catalyst for degradation of volatile organic compounds in the gas phase. Appl. Catal. B **106**(3–4), 445–452 (2011)
127. Zhou, X., et al.: Plasmon-assisted degradation of toxic pollutants with Ag-AgBr/Al_2O_3 under visible-light irradiation. J. Phys. Chem. C **114**(6), 2746–2750 (2010)
128. Begum, G., Manna, J., Rana, R.K.: Controlled orientation in a bio-inspired assembly of Ag/AgCl/ZnO nanostructures enables enhancement in visible-light-induced photocatalytic performance. Chem. Eur. J. **18**(22), 6847–6853 (2012)
129. Cheng, H., et al.: In situ ion exchange synthesis of the novel Ag/AgBr/BiOBr hybrid with highly efficient decontamination of pollutants. Chem. Commun. **47**(25), 7054–7056 (2011)
130. Zhu, Q., et al.: Facile synthesis of the novel Ag_3VO_4/AgBr/Ag plasmonic photocatalyst with enhanced photocatalytic activity and stability. J. Phys. Chem. C **117**(11), 5894–5900 (2013)
131. Cai, B., et al.: Advanced visible-light-driven photocatalyst upon the incorporation of sulfonated graphene. Nanoscale **5**(5), 1910–1916 (2013)
132. Zhang, H., et al.: Graphene sheets grafted Ag@AgCl hybrid with enhanced plasmonic photocatalytic activity under visible light. Environ. Sci. Technol. **45**(13), 5731–5736 (2011)
133. Wang, X., Lim, T.-T.: Highly efficient and stable Ag-AgBr/TiO_2 composites for destruction of Escherichia coli under visible light irradiation. Water Res. **47**(12), 4148–4158 (2013)

134. Wu, T., et al.: Surface plasmon resonance-induced visible light photocatalytic reduction of graphene oxide: Using Ag nanoparticles as a plasmonic photocatalyst. Nanoscale **3**(5), 2142–2144 (2011)
135. Jiang, B., et al.: In situ fabrication of Ag/Ag_3PO_4/graphene triple heterostructure visible-light photocatalyst through graphene-assisted reduction strategy. ChemCatChem **5**(6), 1359–1367 (2013)
136. Hou, Y., et al.: Ag_3PO_4 Oxygen evolution photocatalyst employing synergistic action of Ag/AgBr nanoparticles and graphene sheets. J. Phys. Chem. C **116**, 20132–20139 (2012)
137. Min, Y., et al.: Self-assembled encapsulation of graphene oxide/Ag@AgCl as a Z-scheme photocatalytic system for pollutant removal. J. Mater. Chem. A **2**(5), 1294–1301 (2014)
138. Luo, G., et al.: Facile fabrication and enhanced photocatalytic performance of Ag/AgCl/rGO heterostructure photocatalyst. ACS Appl. Mater. Interfaces **5**(6), 2161–2168 (2013)
139. Ng, Y.H., et al.: To what extent do graphene scaffolds improve the photovoltaic and photocatalytic response of tio2 nanostructured films? J. Phys. Chem. Lett. **1**(15), 2222–2227 (2010)
140. Liang, Q., et al.: Enhanced photocatalytic activity and structural stability by hybridizing Ag_3PO_4 nanospheres with graphene oxide sheets. Phys. Chem. Chem. Phys. **14**(45), 15657–15665 (2012)
141. Liu, L., Liu, J., Sun, D.D.: Graphene oxide enwrapped Ag_3PO_4 composite: towards a highly efficient and stable visible-light-induced photocatalyst for water purification. Catal. Sci. Technol. **2**(12), 2525–2532 (2013)
142. Xiang, Q., Yu, J., Jaroniec, M.: Graphene-based semiconductor photocatalysts. Chem. Soc. Rev. **41**(2), 782–796 (2012)
143. An, X., Yu, J.C.: Graphene-based photocatalytic composites. RSC Adv. **1**(8), 1426–1434 (2011)
144. Ng, Y.H., Iwase, A., Bell, N.J., Kudo, A., Amal, R.: Semiconductor/reduced graphene oxide nanocomposites derived from photocatalytic reactions. Cat. Today **164**(1), 353–357 (2011)
145. Gao, W., et al.: One-pot synthesis of Ag/r-GO/TiO_2 nanocomposites with high solar absorption and enhanced anti-recombination in photocatalytic applications. Nanoscale **6**(10), 5498–5508 (2014)
146. Stamplecoskie, K.G., et al.: Plasmon-mediated photopolymerization maps plasmon fields for silver nanoparticles. J. Am. Chem. Soc. **133**(24), 9160–9163 (2011)
147. Deeb, C., et al.: Plasmon-based free-radical photopolymerization: effect of diffusion on nanolithography processes. J. Am. Chem. Soc. **133**(27), 10535–10542 (2011)
148. Stamplecoskie, K.G., Fasciani, C., Scaiano, J.C.: Dual-stage lithography from a light-driven, plasmon-assisted process: a hierarchical approach to subwavelength features. Langmuir **28**(30), 10957–10961 (2012)
149. Stamplecoskie, K.G. and J.C. Scaiano, Plasmon mediated polymerization on the surface of silver nanoparticles for advancements in photolithographic patterning. Proc. SPIE, Advances in Resist Materials and Processing Technology XXIX, vol 8325, pp. 832527/1–832527/6 (2012)
150. Hubert, C., et al.: Near-Field Photochemical Imaging of Noble Metal Nanostructures. Nano Lett. **5**(4), 615–619 (2005)
151. Yang, X., et al.: Photocatalytic oxidation of methanol to methyl formate in liquid phase over supported silver catalysts. Catal. Commun. **43**, 192–196 (2014)
152. Zhang, D.-H., et al.: One-pot synthesis of Ag-Fe_3O_4 nanocomposite: a magnetically recyclable and efficient catalyst for epoxidation of styrene. Chem. Commun. **29**, 3414–3416 (2008)
153. Duan, S., et al.: Roles of plasmonic excitation and protonation on photoreactions of p-aminobenzenethiol on Ag nanoparticles. J. Phys. Chem. C **118**(13), 6893–6902 (2014)
154. Zhao, L.-B., et al.: Theoretical study of plasmon-enhanced surface catalytic coupling reactions of aromatic amines and nitro compounds. J. Phys. Chem. Lett. **5**(7), 1259–1266 (2014)
155. Huang, Y.-F., et al.: When the signal is not from the original molecule to be detected: chemical transformation of para-aminothiophenol on Ag during the SERS measurement. J. Am. Chem. Soc. **132**(27), 9244–9246 (2010)
156. Sun, M., et al.: Activated vibrational modes and fermi resonance in tip-enhanced Raman spectroscopy. Phys. Rev. E **87**(2), 020401 (2013)

157. Canpean, V., Iosin, M., Astilean, S.: Disentangling SERS signals from two molecular species: A new evidence for the production of p,p,dimercaptoazobenzene by catalytic coupling reaction of p-aminothiophenol on metallic nanostructures. Chem. Phys. Lett. **500**(4−6), 277–282 (2010)
158. Huang, Y., et al.: Can p, p,-Dimercaptoazobisbenzene be produced from p-Aminothiophenol by surface photochemistry reaction in the junctions of a Ag nanoparticle-molecule-Ag (or Au) Film? J. Phys. Chem. C **114**(42), 18263–18269 (2010)
159. Xu, P., et al.,: Mechanistic understanding of surface plasmon assisted catalysis on a single particle: cyclic redox of 4-aminothiophenol. Sci. Rep.**3** (2013)
160. Sun, M., et al.: The pH-controlled plasmon-assisted surface photocatalysis reaction of 4-Aminothiophenol to p,p´-Dimercaptoazobenzene on Au, Ag, and Cu colloids. J. Phys. Chem. C **115**(19), 9629–9636 (2011)
161. Sun, M., et al.: Remote excitation polarization-dependent surface photochemical reaction by plasmonic waveguide. Plasmonics **6**(4), 681–687 (2011)
162. Sun, M., Hou, Y., Xu, H.: Can information of chemical reaction propagate with plasmonic waveguide and be detected at remote terminal of nanowire? Nanoscale **3**(10), 4114–4116 (2011)
163. Busch, D.G., Ho, W.: Direct observation of the crossover from single to multiple excitations in femtosecond surface photochemistry. Phys. Rev. Lett. **77**, 1338–1341 (1996)
164. Bonn, M., et al.: Phonon- versus electron-mediated desorption and oxidation of CO on Ru(0001). Science **285**(5430), 1042–1045 (1999)
165. Denzler, D.N., et al.: Electronic excitation and dynamic promotion of a surface reaction. Phys. Rev. Lett. **91**(22), 226102 (2003)
166. Buntin, S.A., et al.: Optically driven surface reactions: evidence for the role of hot electrons. Phys. Rev. Lett. **61**(11), 1321–1324 (1988)
167. Olsen, T., Gavnholt, J., Schiøtz, J.: Hot-electron-mediated desorption rates calculated from excited-state potential energy surfaces. Phys. Rev. B **79**(3), 035403 (2009)
168. Olsen, T., Schitøz, J.: Origin of power laws for reactions at metal surfaces mediated by hot electrons. Phys. Rev. Lett. **103**(23), 238301 (2009)
169. Wingreen, N.S., Jacobsen, K.W., Wilkins, J.W.: Inelastic scattering in resonant tunneling. Phys. Rev. B **40**(17), 11834–11850 (1989)
170. Kim, K.H., et al.: Enhanced photoinduced desorption from metal nanoparticles by photoexcitation of confined hot electrons using femtosecond laser pulses. Phys. Rev. Lett. **107**, 047401 (2011)
171. Mulugeta, D., et al.: Size effects in thermal and photochemistry of $(NO)_2$ on Ag nanoparticles. Phys. Rev. Lett. **101**, 146103 (2008)
172. Phillips, K.R., et al.: Sequential photo-oxidation of methanol to methyl formate on TiO2(110). J. Am. Chem. Soc. **135**, 574–577 (2013)
173. Fang, Y., et al.: Ascertaining p, p, Dimercaptoazobenzene produced from p-Aminothiophenol by selective catalytic coupling reaction on silver nanoparticles. Langmuir **26**(11), 7737–7746 (2010)
174. Ingram, D.B., Linic, S.: Water splitting on composite plasmonic-metal/semiconductor photoelectrodes: evidence for selective plasmon-induced formation of charge carriers near the semiconductor surface. J. Am. Chem. Soc. **133**(14), 5202–5205 (2011)
175. Sun, T., et al.: High photocatalytic activity of hydrogen production from water over Fe doped and Ag deposited anatase TiO_2 catalyst synthesized by solvothermal method. Chem. Eng. J. **228**, 896–906 (2013)
176. Wei, Y., et al.: Polydopamine-assisted decoration of ZnO nanorods with Ag nanoparticles: an improved photoelectrochemical anode. J. Mater. Chem. A **1**(16), 5045–5052 (2013)
177. Solarska, R., Krolikowska, A., Augustynski, J.: Silver nanoparticle induced photocurrent enhancement at WO_3 photoanodes. Angew. Chem. Int. Ed. **49**(43), 7980–7983 (2010)
178. Chuang, H.-Y., Chen, D.-H.: Fabrication and photoelectrochemical study of Ag@TiO_2 nanoparticle thin film electrode. Int. J. Hydrogen Energy **36**(16), 9487–9495 (2011)
179. Wei, Y., et al.,: Enhanced photoelectrochemical water-splitting effect with a bent ZnO nanorod photoanode decorated with Ag nanoparticles. Nanotechnology, **23**(23), 235401/1–235401/8 (2012)